

# Analytical Methods

Accepted Manuscript



This is an *Accepted Manuscript*, which has been through the Royal Society of Chemistry peer review process and has been accepted for publication.

*Accepted Manuscripts* are published online shortly after acceptance, before technical editing, formatting and proof reading. Using this free service, authors can make their results available to the community, in citable form, before we publish the edited article. We will replace this *Accepted Manuscript* with the edited and formatted *Advance Article* as soon as it is available.

You can find more information about *Accepted Manuscripts* in the [Information for Authors](#).

Please note that technical editing may introduce minor changes to the text and/or graphics, which may alter content. The journal's standard [Terms & Conditions](#) and the [Ethical guidelines](#) still apply. In no event shall the Royal Society of Chemistry be held responsible for any errors or omissions in this *Accepted Manuscript* or any consequences arising from the use of any information it contains.

# Electrochemiluminescence Sensor based on Sulfur-Terminal CdS<sub>2</sub>L Complex

Chunyan Zhang, Lei Wang, Shengyi Zhang\*, Changjie Mao, Jiming Song, Helin Niu,

Baokang Jin, Yupeng Tian

Department of Chemistry, Anhui University, Hefei 230601, China

\*Corresponding author. E-mail: syzhang@126.com

**Abstract:** The electrochemiluminescence (ECL) behavior of the sulfur-terminal CdS<sub>2</sub>L complex as-synthesized was studied, and the ECL mechanism and effect factors were discussed. Based on strong and stable ECL emission of the CdS<sub>2</sub>L complex, a solid-state ECL sensor was fabricated. The sensor as-prepared was used to detect glutathione (GSH), and the results show that the linear response range is from 0.002  $\mu$ M to 4  $\mu$ M with a detection limit of 0.67 nM for GSH solution.

**Keywords:** CdS<sub>2</sub>L Complex; Electrochemiluminescence; Sensor; Glutathione

## 1. Introduction

Through ideal combination of electrochemical and spectroscopic methods, the electrochemiluminescence (ECL) shows outstanding advantages over photoluminescence (PL) and chemiluminescence (CL), due to its versatility, simplified optical setup, good temporal and spatial control [1-3]. The ECL is a redox-induced light emission in which species generated at electrode undergo high energy electron transfer reaction to form excited states and then emit light. In transformation from electrical energy into radiative energy, the ECL active materials (or ECL precursors) that can be excited to the intermediates play a key role. Early, some CL active materials such as luminol and ruthenium(II) complex, were used as

1  
2  
3 ECL active materials that promoted the development of ECL technique [4-8].  
4  
5 Recently, inorganic nanoparticles such as CdSe [9, 10], CdTe [11, 12] and CdS [13,  
6  
7 14], have been introduced to ECL system, because of their controllable size and  
8  
9 emission wavelength, good chemical stability and low cost. However, weak ECL  
10  
11 signals and poor biocompatibility of the inorganic nanoparticles limit their  
12  
13 applications in ECL fields. In order to improve the ECL property of inorganic  
14  
15 nanoparticles, many works pay much attention to investigating inorganic-organic  
16  
17 hybrid materials. For example, Ju et al. prepared the carbohydrate-functionalized CdS  
18  
19 nanocomposite that was used as ECL biosensor [15]. Wu et al. developed a strategy  
20  
21 for the construction of ECL sensor in which CdS quantum dots were combined with  
22  
23 polyamidoamine and gold nanoparticles [16]. Our group reported an ECL  
24  
25 immunosensor that was fabricated by graphene oxide nanosheets/polyaniline  
26  
27 nanowires/CdSe quantum dots nanocomposite [17].  
28  
29  
30

31  
32 The two-photon absorption (TPA) is one of the most important reverse saturable  
33  
34 absorption behaviors, and the TPA active material that can absorb two photons in  
35  
36 excitation process, is a kind of nonlinear optical materials. Similar to the development  
37  
38 of the ECL active materials, the TPA active materials have been developed from  
39  
40 inorganic and organic species to inorganic-organic hybrid materials [18-19]. Our  
41  
42 group reported a novel sulfur-terminal complex  $\text{CdS}_2\text{L}$  (L=N-hexyl-3-{2-[4-  
43  
44 (2,2':6',2''-terpyridin-4'-yl)phenyl]-ethenyl}-carbazole) with TPA activity in the  
45  
46 near-infrared region [20]. In this paper, the ECL activity of the  $\text{CdS}_2\text{L}$  complex was  
47  
48 studied and the possible pathway for the ECL emission of the  $\text{CdS}_2\text{L}$  complex/ $\text{S}_2\text{O}_8^{2-}$   
49  
50 system was discussed. In addition, the solid-state ECL biosensor fabricated with  
51  
52  $\text{CdS}_2\text{L}$  complex was used to detect glutathione (GSH), and satisfactory results were  
53  
54 obtained.  
55  
56  
57  
58  
59  
60

## 2. Experimental

### 2.1 Materials and instruments

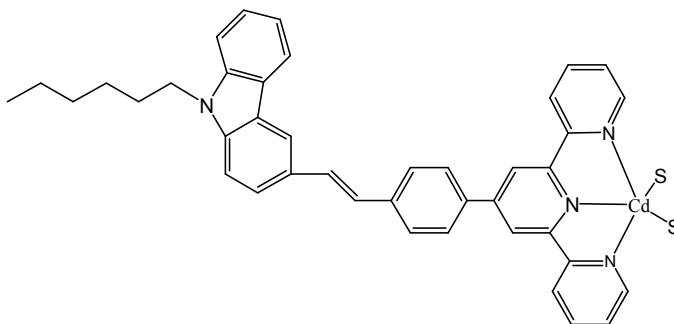
Main Materials: Cadmium powder (99%), sodium thiocyanate (AR), ethylenediamine (99%), ethyl alcohol (99.7%), tri-n-propylamine (TPrA, CP) and N,N-dimethyl formamide (DMF, 99%) were purchased from Sinopharm Chemical Reagent Co., Ltd. Sulfur powder (99%) was obtained from Tianjin Baishi Chemical Industry Co., Ltd. Glutathione (GSH, >98%) was bought from Shanghai Sangon Biotech Co., Ltd. Nafion was purchased from Sigma Aldrich. All reagents were used as obtained without further purification. The phosphate buffer solutions with different pH values were prepared by mixing 0.1 M Na<sub>2</sub>HPO<sub>4</sub> and 0.1 M NaH<sub>2</sub>PO<sub>4</sub> according to different volume ratio. The solutions were prepared with ultrapure water.

Main instruments: Fluorescence spectrophotometer (FL, LS-55, PerkinElmer); Electrochemical workstations (IM6, ZAHNER, Germany; CHI660E, Shanghai Chenhua Instruments Ltd); Electrochemiluminescence analyzer (RFL-1, Xi'An Remex Analyse Instrument Co., Ltd, China. The spectral width and voltage of the photomultiplier tube were set at 200-800 nm and 600 V, respectively); Ultrasonic cleaner (KQ-50E, Kunshan ultrasonic instrument Co., Ltd).

### 2.2 Synthesis of CdS<sub>2</sub>L complex

The synthesis of CdS<sub>2</sub>L complex was performed according to the solvothermal procedure reported by our group [20]. First, the ligand L was synthesized by the solvent free Wittig reaction and the CdS nanocrystals were prepared by reacting sulfur powder with cadmium powder in ethylenediamine at 130°C. Then, the CdS<sub>2</sub>L complex was prepared by reacting CdS nanocrystals with L and sodium thiocyanate in ethyl alcohol at 130°C. In addition, for comparison, the L-capped CdS nanocrystals were synthesized by reacting sulfur powder with cadmium powder and L in

1  
2  
3 ethylenediamine at 130°C.  
4  
5



18  
19  
20  
21  
22  
23  
24  
25  
26  
27  
28  
29  
30  
31  
32  
33  
34  
35  
36  
37  
38  
39  
40  
41  
42  
43  
44  
45  
46  
47  
48  
49  
50  
51  
52  
53  
54  
55  
56  
57  
58  
59  
60

**Scheme 1.** Structure of CdS<sub>2</sub>L complex

### 2.3 Assembly of sensor

First, the surface of the Au electrode was polished by 1.0, 0.3 and 0.05 μm α-Al<sub>2</sub>O<sub>3</sub> powder successively, and cleaned by sonicated in water and C<sub>2</sub>H<sub>5</sub>OH in turn for 2 min. Then, the cleaned Au electrode was scanned between -0.5 V and 1.5 V at 100 mV/s in 0.5 M H<sub>2</sub>SO<sub>4</sub> until a reproducible cyclic voltammogram (CV) was obtained. After washing with water and drying in N<sub>2</sub> flow, the surface of the Au electrode was modified with 3 μL CdS<sub>2</sub>L complex solution (0.5 mg/mL in DMF) and dried at room temperature. For comparison, 3 μL L-capped CdS nanocrystals solution (0.5 mg/mL in DMF) was also modified on the surface of the Au electrode. Finally, the sensor was obtained by overlaying 2 μL 0.1% Nafion ethanol solution on the surface of the modified electrode.

### 2.4 Measurements

In measurements, three-electrode system was used: the modified Au electrode as work electrode, an Ag/AgCl as reference electrode and a platinum wire as counter electrode. Typically, the ECL tests were performed by cyclic voltammetric (CV) scanning between 0 and -1.6 V at 200 mV/s in 0.1 M PBS (pH7.4) solution containing 0.1 M KCl and 0.1 M K<sub>2</sub>S<sub>2</sub>O<sub>8</sub>.

## 3. Results and discussion

### 3.1 ECL Behavior and mechanism

The ECL behavior of the products was studied and the results were shown in Fig.1A. From the patterns, it is observed that the ECL intensity of CdS<sub>2</sub>L complex is highest among three products. In addition, as shown in Fig.1B, the strong ECL emission of CdS<sub>2</sub>L complex could keep constant almost when successive potential scans were carried out.

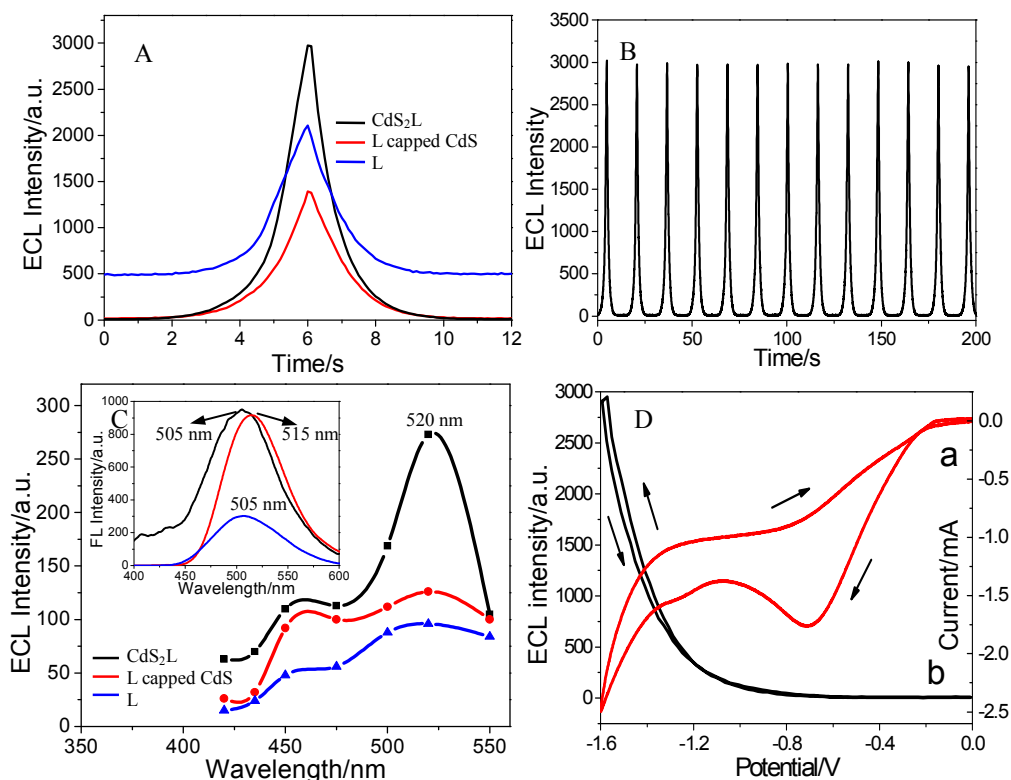
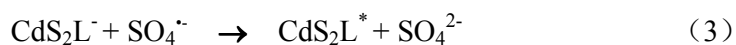
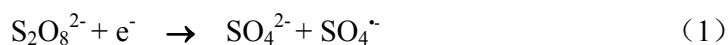


**Fig.1** (A) ECL-potential curves obtained by the electrodes modified with different products; (B) Repeated ECL emissions along with successive CV scans on electrode modified with CdS<sub>2</sub>L complex; (C) ECL spectra (obtained by optical filters with wave length width 25 nm) of the products (insert: FL spectra obtained by exciting at 310 nm); (D) Relationship of CV curve (a) and ECL curve (b) of the electrode modified with CdS<sub>2</sub>L complex.

The ECL and FL spectra of the products are shown in Fig.1C. From FL spectra, it is observed that the FL emission peak produced by L-capped CdS nanocrystals is

1  
2  
3 located at longer wavelength (515 nm) comparing with other products. As well known,  
4  
5 for small organic molecules that have been excited, the FL emission resulted from the  
6  
7 electron transition from highest occupied molecular orbital (HOMO) to lowest  
8  
9 unoccupied molecular orbital (LUMO). However, for nanocrystals, the FL emission  
10  
11 comes from the hole-electron recombinations. This difference of FL emission  
12  
13 mechanism made the FL peak of L-capped CdS nanocrystals located at longer  
14  
15 wavelength, according to the results reported [20]. From ECL spectra of three  
16  
17 products, it is seen that there is no obvious difference in peak location. For CdS<sub>2</sub>L  
18  
19 complex, the ECL emission peak red-shifted comparing with the peak location of FL  
20  
21 emission, which is explained as follows. In principle, the ECL emission depended on  
22  
23 the surface property of modified electrode. Perhaps, the CdS<sub>2</sub>L molecules adsorbed on  
24  
25 the surface of electrode have smaller energy level difference than that in solution.  
26  
27  
28

29  
30 From the relationship of the ECL curve with the CV curve for the electrode  
31  
32 modified with CdS<sub>2</sub>L complex, as shown in Fig.1D, it is observed that there is a  
33  
34 strong cathodic peak at -0.70 V on CV curve. During negative scanning from -1.2 V  
35  
36 to -1.6 V, the cathodic current increased rapidly meanwhile the ECL emission  
37  
38 enhanced quickly. Based on these results and by analogy with the known  
39  
40 complex/S<sub>2</sub>O<sub>8</sub><sup>2-</sup> ECL systems [21], the ECL mechanism of CdS<sub>2</sub>L complex/S<sub>2</sub>O<sub>8</sub><sup>2-</sup>  
41  
42 system is proposed as follows:  
43



51  
52  
53  
54  
55 First, the coreactant S<sub>2</sub>O<sub>8</sub><sup>2-</sup> in solution diffused to the surface of electrode and was  
56  
57 reduced to the strong oxidant SO<sub>4</sub><sup>·-</sup> by electrode reaction (1), which formed a cathodic  
58  
59  
60

1  
2  
3 peak at -0.7 V on CV curve [22]. Then, the CdS<sub>2</sub>L complex was reduced by electrode  
4  
5 reaction (2), which produced large cathodic current during negative scanning from  
6  
7 -1.2 V to -1.6 V. As reported [23], the SO<sub>4</sub><sup>•-</sup> is a strong oxidant, which has a redox  
8  
9 potential of E<sup>0</sup> ≥ +3.15 V versus SCE. Therefore, by means of the oxidative reaction (3)  
10  
11 of SO<sub>4</sub><sup>•-</sup> with the CdS<sub>2</sub>L<sup>-</sup>, the excited state CdS<sub>2</sub>L<sup>\*</sup> species were produced. Finally,  
12  
13 strong ECL emission was produced by way of the release of the photons while  
14  
15 CdS<sub>2</sub>L<sup>\*</sup> species returned to their ground state as shown in photochemical reaction (4).  
16  
17

18  
19 From Fig.1A, it is seen that the ECL emission of ligand L itself was enhanced due  
20  
21 to the formation of CdS<sub>2</sub>L complex that has lower activation energy and higher  
22  
23 luminous efficiency than ligand L, presumably. In our previous work [20], it has been  
24  
25 demonstrated that the TPA cross section (σ) of L-capped CdS nanocrystals is 1.5-fold  
26  
27 as high as that of CdS<sub>2</sub>L complex. Here, the ECL intensity of CdS<sub>2</sub>L complex is about  
28  
29 twice as high as that of L-capped CdS nanocrystals, which is explained as follows.  
30  
31 According to the results reported [20], the L-capped CdS nanocrystals have an  
32  
33 electron and energy redistribution between capping L and CdS nanocrystals, which  
34  
35 exhibited higher TPA activity comparing with CdS<sub>2</sub>L complex. However, for  
36  
37 L-capped CdS nanocrystals, this redistribution that was in favour of absorption to  
38  
39 optical energy (namely two-photon absorption) may be an adverse factor for ECL  
40  
41 emission that is the releasing process of energy. Therefore, the ECL activity of  
42  
43 L-capped CdS nanocrystals is lower than that of CdS<sub>2</sub>L complex.  
44  
45

### 46 47 3.2 Effect factors on ECL behavior of CdS<sub>2</sub>L complex

48  
49 For the electrode modified with CdS<sub>2</sub>L complex, the effect factors on ECL behavior  
50  
51 were studied and the results are shown in Fig.2. As reported [12], high potential scan  
52  
53 rate can enrich excited state CdS<sub>2</sub>L<sup>\*</sup> species on electrode surface in a short time span  
54  
55 and thus enhance ECL emission. For our ECL system, as shown in Fig.2A, the ECL  
56  
57  
58  
59  
60

intensity enhanced when the scan rate was increased from 100 to 200 mV/s. However, if the scan rate was increased to 300 mV/s, the ECL intensity decreased, which is explained as that the electrode reaction of coreactant  $S_2O_8^{2-}$  could not catch up with the scan rate [24]. Therefore, the scan rate was set at 200 mV/s for ECL emission of  $CdS_2L$  complex. Fig.2B shows the effect of  $CdS_2L$  mass on ECL intensity. From the pattern, it is observed that the ECL intensity enhanced rapidly along with the increase of  $CdS_2L$  mass in the beginning, and reached a maximum value at 1.5  $\mu g$ . Nevertheless, superfluous  $CdS_2L$  could not improve the ECL emission, since the accumulated  $CdS_2L$  would physically block the emission light reaching the photomultiplier detector, resulting in the decrease of detected ECL intensity [25]. From Fig.2C that shows the effect of electrolyte acidity on ECL intensity, it is noticed that the ECL intensity enhanced along with the increase of pH value from 5 to 7.4, and decreased when the pH value exceeded 7.4. In other words, maximum ECL intensity occurred at around neutral solution. In alkalic solution, the decrease of ECL intensity could be attributed to the consumption of  $SO_4^{\cdot-}$  by reacting with  $OH^-$  [26].



In acidic solution, the ECL emission was weakened due to the consumption of  $CdS_2L^-$  by reacting with  $H_3O^+$  [23]:



In addition, the conjugate acid  $CdS_2LH^+$  of  $CdS_2L$  complex may be formed in acidic solution, which consumed  $CdS_2L^-$ . As shown insert in Fig.2C, perhaps, the cathodic peak at about -1.3 V on CV curve obtained in pH5 solution originated from the electrode process of  $CdS_2LH^+$ :



Here, the continuous release of  $H_2$  produced by reactions (6) and (7) could lower

the ECL intensity, due to its interference to the reactions and mass transfer on the electrode surface.

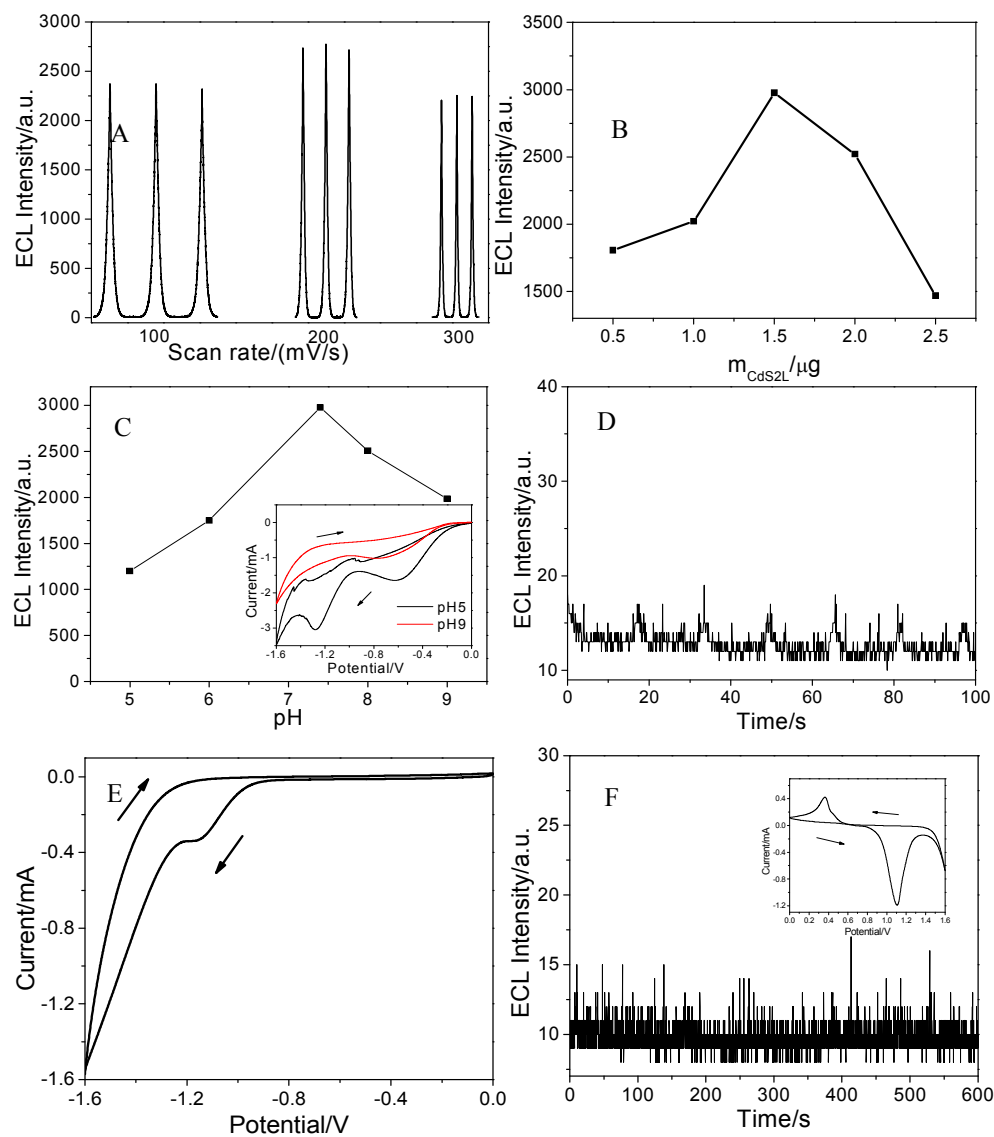


**Fig.2** ECL behavior of CdS<sub>2</sub>L complex in different conditions: (A) at different potential scan rates; (B) with different CdS<sub>2</sub>L mass; (C) in electrolyte solutions with different pH value (insert: CV curves); (D) in PBS solution (pH7.4) without K<sub>2</sub>S<sub>2</sub>O<sub>8</sub>; (E) CV curve in PBS solution (pH7.4) without K<sub>2</sub>S<sub>2</sub>O<sub>8</sub>; (F) in PBS solution (pH7.4) containing 1mM TPrA (insert: CV curve).

In 0.1 M PBS solution without K<sub>2</sub>S<sub>2</sub>O<sub>8</sub>, very weak ECL signal was produced

1  
2  
3 (Fig.2D) and there was only a reduction peak of CdS<sub>2</sub>L complex on CV curve  
4  
5 (Fig.2E). Clearly, the coreagent K<sub>2</sub>S<sub>2</sub>O<sub>8</sub> played an important role in ECL process.  
6  
7 When the K<sub>2</sub>S<sub>2</sub>O<sub>8</sub> was replaced by TPrA, as shown in Fig.2F, there was no ECL signal  
8  
9 during potential scanning from 0 to 1.6 V. As well known, in ECL system, K<sub>2</sub>S<sub>2</sub>O<sub>8</sub> is a  
10  
11 reductive-oxidation coreactant while TPrA is an oxidation-reductive coreactant [27].  
12  
13 Here, the CdS<sub>2</sub>L/TPrA system has no ECL emission during positive-potential  
14  
15 scanning, which is explained that the oxidation reaction of CdS<sub>2</sub>L complex is difficult  
16  
17 to take place. Therefore, there are only redox peaks of TPrA on the CV curve, as  
18  
19 shown insert in Fig.2F.  
20  
21

#### 22 23 4. ECL analysis

24  
25 As above, the CdS<sub>2</sub>L complex produced strong and stable ECL emission in  
26  
27 presence of K<sub>2</sub>S<sub>2</sub>O<sub>8</sub>, which is the basis of ECL sensor. In addition, the CdS<sub>2</sub>L complex  
28  
29 has good biological compatibility due to its terminal sulfur atoms. Therefore, the  
30  
31 electrode modified with CdS<sub>2</sub>L complex was used as ECL sensor for biomolecule  
32  
33 GSH detection. The GSH, as an important tripeptide consisted of glutamate, cysteine  
34  
35 and glycine, exists in almost all living cells and takes part in main biochemical  
36  
37 reactions as reductant. Therefore, the detection of GSH is significant in biological  
38  
39 science [28]. From the test results shown in Fig.3A, it is concluded that the ECL  
40  
41 intensity of the sensor responded to GSH concentration, sensitively. Consulting the  
42  
43 literature [29], this response resulted from the quenching mechanism of GSH to ECL  
44  
45 emission, due to the formation of S...H hydrogen bonding between CdS<sub>2</sub>L and GSH.  
46  
47 Fig.3B shows the change of the ECL intensity along with the increase of GSH  
48  
49 concentration. Based on the relationship between ECL intensity and logarithm of  
50  
51 GSH concentration (insert in Fig.3B), it is obtained that the linear range of the sensor  
52  
53 for GSH detection is from 0.002μM to 4μM (R=0.9956) and the detection limit is 0.67  
54  
55  
56  
57  
58  
59  
60

nM (S/N=3). Comparing with the results reported in literature [29], our sensor has lower detection limit to GSH detection. In addition, it was found that 2  $\mu\text{M}$  cysteine had no interference to GSH detection, although cysteine has similar functional groups (e.g., -SH, -COOH and  $-\text{NH}_2$ ) to GSH. Consulting literature [29], the phenomenon is explained as that the hydrogen bonding energy between  $\text{CdS}_2\text{L}$  and GSH much less than that between  $\text{CdS}_2\text{L}$  and cysteine.

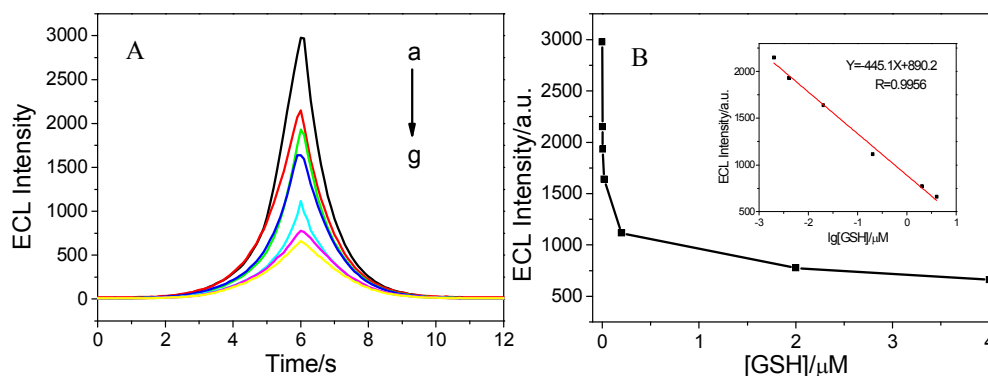


**Fig.3** (A) ECL intensity changes vs GSH concentrations ( $\mu\text{M}$ ): (a) 0; (b) 0.002; (c) 0.004; (d) 0.0 2; (e) 0.2; (f) 2; (g) 4. (B) Relationship between ECL intensity and GSH concentration (Insert: calibration curve of the ECL intensity vs logarithmic GSH concentrations).

## 5. Conclusion

In summary, using sulfur powder, cadmium powder and ligand L as precursors, sulfur-terminal  $\text{CdS}_2\text{L}$  complex was prepared. The ECL property and mechanism of the  $\text{CdS}_2\text{L}/\text{S}_2\text{O}_8^{2-}$  system were studied. A series of comparison tests, such as ECL emission with FL emission, ECL property with TPA property,  $\text{CdS}_2\text{L}$  complex with L-capped CdS nanocrystals and  $\text{CdS}_2\text{L}/\text{S}_2\text{O}_8^{2-}$  system with  $\text{CdS}_2\text{L}/\text{TPrA}$  system, were performed. Based on the excellent ECL property of  $\text{CdS}_2\text{L}/\text{S}_2\text{O}_8^{2-}$  system, the ECL sensor was constructed with  $\text{CdS}_2\text{L}$  complex. The linear range of the sensor for GSH detection is from 0.002  $\mu\text{M}$  to 4  $\mu\text{M}$  and the detection limit is 0.67 nM. Significantly, present work in which the  $\text{CdS}_2\text{L}$  complex with TPA activity was used in ECL system,

would open up a new use field for TPA materials.

## Acknowledgments

This work was supported by grants from the National Natural Science Foundation of China (Nos.21275006, 21471001, 20905001, 21071002, 21175001, 51432001).

## References

- [1] M. M. Richter, *Chem. Rev.*, 2004, 104, 3003-3036.
- [2] W. Miao, *Chem. Rev.*, 2008, 108, 2506-2553.
- [3] E. Rampazzo, S. Bonacchi, D. Genovese, R. Juris, M. Marcaccio, M. Montalti, F. Paolucci, M. Sgarzi, G. Valenti, N. Zaccheroni, L. Prodi, *Coordin. Chem. Rev.*, 2012, 256, 1664-1681.
- [4] H. Cui, G. Zou, X. Lin, *Anal. Chem.*, 2003, 75, 324-331.
- [5] Y. Dong, H. Cui, Y. Xu, *Langmuir*, 2007, 23, 523-529.
- [6] Y. Cao, R. Yuan, Y. Chai, L. Mao, H. Niu, H. Liu, Y. Zhuo, *Biosens. Bioelectron.*, 2012, 31, 305-309.
- [7] R. D. Gerardi, N. W. Barnett, S. W. Lewis, *Anal. Chim. Acta*, 1999, 378, 1-41.
- [8] J. Xia, S. Ding, B. Gao, Y. Sun, Y. Wang, S. Cosnier, X. Guo, *J. Electroanal. Chem.*, 2013, 692, 60-65.
- [9] G. Jie, J. Zhang, D. Wang, C. Cheng, H. Chen, *J. Zhu, Anal. Chem.*, 2008, 80, 4033-4039.
- [10] T. Wang, S. Zhang, C. Mao, J. Song, H. Niu, B. Jin, Y. Tian, *Biosens. Bioelectron.*, 2012, 31, 369-375.
- [11] Y. Shan, J. Xu, H. Chen, *Chem. Commun.*, 2010, 46, 5079-5081.
- [12] H. Liang, D. Song, J. Gong, *Biosens. Bioelectron.*, 2014, 53, 363-369.
- [13] Y. Zhang, H. Zhou, P. Wu, H. Zhang, J. Xu, H. Chen, *Anal. Chem.*, 2014, 86, 8657-8664.
- [14] J. Wang, Y. Shan, W. Zhao, J. Xu, H. Chen, *Anal. Chem.*, 2011, 83, 4004-4011.
- [15] E. Han, L. Ding, S. Jin, H. Ju, *Biosens. Bioelectron.*, 2011, 26, 2500-2505.
- [16] F. Sun, F. Chen, W. Fei, L. Sun, Y. Wu, *Sensors and Actuators B*, 2012, 166-167, 702-707
- [17] P. Liu, X. Hu, C. Mao, H. Niu, J. Song, B. Jin, S. Zhang, *Electrochim. Acta*, 2013, 113

- 1  
2  
3 176-180.  
4  
5 [18] G. He, L. Tan, Q. Zheng, P. Prasad, *Chem. Rev.*, 2008, 108, 1245-1330.  
6  
7 [19] G. Thomas, J. Voskuilen, H. C. Gerritsen, H.J.C.M. Sterenborg, *Journal of Photochemistry*  
8  
9 *and Photobiology B: Biology*, 2014, 141, 128-138.  
10  
11 [20] Q. Zhang, Y. Gao, S. Zhang, J. Wu, H. Zhou, J. Yang, X. Tao, Y. Tian, *Dalton Trans.*, 2012,  
12  
13 41, 7067-7072.  
14  
15 [21] Z. Chen, K. M. C. Wong, E. C. H. Kwok, N. Zhu, Y. Zu, V. W. W. Yam, *Inorg. Chem.*, 2011,  
16  
17 50, 2125-2132.  
18  
19 [22] G. Jie, H. Huang, X. Sun, J. Zhu, *Biosens. Bioelectron.*, 2008, 23, 1896-1899.  
20  
21 [23] R. Memming, *J. Electrochem. Soc.*, 1969, 116, 785-793.  
22  
23 [24] Y. Wen, F. Luo, Y. Yang, L. Lin, J. Du, Y. Guo, D. Xiao, M. M. F. Choi, *Anal. Methods*, 2012,  
24  
25 4, 1053-1059.  
26  
27 [25] K. Komori, K. Takada, O. Hatozaki, N. Oyama, *Langmuir*, 2007, 23, 6446-6452.  
28  
29 [26] K. Yamashita, S. Yamazaki-Nishida, Y. Harima, A. Segawa, *Anal. Chem.*, 1991, 63, 872-876.  
30  
31 [27] H. Li, J. Chen, S. Han, W. Niu, X. Liu, G. Xu, *Talanta*, 2009, 79, 165-170.  
32  
33 [28] H. Sies, *Free Radical Biol. Med.*, 1999, 27, 916-921.  
34  
35 [29] Y. Wang, J. Lu, L. Tang, H. Chang, J. Li, *Anal. Chem.*, 2009, 81, 9710-9715.  
36  
37  
38  
39  
40  
41  
42  
43  
44  
45  
46  
47  
48  
49  
50  
51  
52  
53  
54  
55  
56  
57  
58  
59  
60

## Graphical Abstract

Sulfur-terminal CdS<sub>2</sub>L complex was synthesized by solvothermal reaction, and its electrochemiluminescence (ECL) property was studied. By comparing both the ECL property with two photon absorption property and CdS<sub>2</sub>L complex with L-capped CdS nanocrystals, the ECL mechanism of the CdS<sub>2</sub>L/S<sub>2</sub>O<sub>8</sub><sup>2-</sup> system was discussed. A solid-state ECL sensor was fabricated with CdS<sub>2</sub>L complex and the detection results show that the liner range is from 0.002 μM to 4 μM and the detection limit is 0.67 nM for GSH.

